Modeling Ion Channel Delays with Fractional Calculus Reveals Early Afterdepolarizations Mechanisms

Noemi Zeraick Monteiro[1], Rodrigo W dos Santos[1], Sandro R Mazorche[1]

[1] Federal University of Juiz de Fora, Juiz de Fora, Brazil

Abstract

Studying the impact of historical factors on ion channel kinetics is essential for understanding complex phenomena in cardiac electrophysiology, such as early afterdepolarizations (EADs), abnormal depolarizations during the action potential plateau associated with life-threatening arrhythmias. Traditional two-variable models without memory mechanisms struggle to accurately replicate EADs. A mathematical framework was developed by incorporating gamma Mittag-Leffler distributed delays and utilizing tools from Fractional Calculus to extend FitzHugh-Nagumo-type models. The approach was applied to a FitzHugh-Nagumo-type model for cardiac cells to generate EADs. The emergence of these oscillations was studied by analyzing characteristics of the memory kernels, such as their mean and variance. The system's stability was also examined. The potential utility of memory kernels in investigating EADs in simplified cardiac models was highlighted.

1.   Introduction

Early afterdepolarizations (EADs) are abnormal depolarizations that occur during the plateau phase of the cardiac action potential (AP) and are associated with life-threatening arrhythmias. Understanding waiting times and time delays in biological processes, including ion channel kinetics, is crucial for comprehending complex phenomena like arrhythmias. Studying EADs in simplified cardiac models is an important research focus, as demonstrated in a recent study [1], that investigates the emergence and evolution of EADs in a reduced three-variable Luo-Rudy model. Two-variable models struggle to replicate EADs due to their reduced dynamical complexity.

In Section 2, we explore the relationship between equations of the form:

$$\frac{dw}{dt} = \frac{w_\infty(u) - w}{\tau_w(u)} \qquad (1)$$

and memory kernels.

Unlike conventional integer-order operators, fractional derivatives are nonlocal and can consider the impact of pre-

vious states or events. This makes them suitable for modeling dynamic systems with memory. The current study explores the generation of EADs by modifying the memory kernel of the slow variable in two-dimensional models using tools from Fractional Calculus (FC).

This approach of constructing general fractional models, discussed in [2,3], is groundbreaking in cardiac modeling. It is applied to a FitzHugh-Nagumo (FHN) model adapted for cardiac phenomena, and insights into the emergence of EADs through the manipulation of memory kernels and stability observations are provided subsequently.

2.   Methods

When analyzing a function y, it can be crucial to consider past states. Delays can be modeled as a Volterra convolution between a memory kernel κ and y, expressed as:

$$\int_0^t \kappa(s)y(t-s)ds = \int_0^t \kappa(t-s)y(s)ds. \qquad (2)$$

A generalized gamma Mittag–Leffler probability distribution function can be considered as a memory kernel:

$$\kappa(t) = \begin{cases} Ct^{\beta-1}e^{-at}E_{\alpha,\beta}(-\lambda t^\alpha), & t \geq 0 \\ 0, & \text{elsewhere,} \end{cases} \qquad (3)$$

where $C = a^\beta + a^{\beta-\alpha}\lambda$ is a normalizing factor, and one of the hypotheses described in [2] must hold. This distribution function encompasses the exponential, gamma and Mittag-Leffler distributions as particular cases.

Properties of FC lead to a comprehensive formulation for the convolution (2) as shown in the equations:

$$\int_0^t \kappa(t-s)y(s)ds = Ce^{-at}D^{1-\beta}(e^{at}w), \qquad (4)$$

$$\frac{dw}{dt} = y - \lambda e^{-at}D^{1-\alpha}(e^{at}w) - aw. \qquad (5)$$

2.1.   Fractionalization of FHN-type systems

In an FHN-type system of differential equations, the fast variable u is referred to as the excitation variable, while the

slow variable w is known as the recovery variable:

$$\frac{du}{dt} = f(u,w), \qquad \frac{dw}{dt} = \frac{w_\infty(u) - w}{\tau_w(u)}. \qquad (6)$$

The special case $\tau_w(u) \equiv \tau$ is related to [4]:

$$w = \int_0^t \frac{1}{\tau} \exp\left(-\frac{1}{\tau}(t-s)\right) w_\infty(u(s))ds. \qquad (7)$$

Eq. (1) implicitly relates to a memoryless exponential delay kernel. We write the convolution with a general delay kernel κ:

$$w = \int_0^t \kappa(t-s)w_\infty(u(s))ds. \qquad (8)$$

Particularly, if $\kappa = \delta_\tau$, the differential system (6) turns into a delayed differential equation (DDE).

We can generalize this model by using the gamma Mittag-Leffler PDF (3) as a distributed delay kernel in Eq. (8), resulting in a general FHN-type fractional model:

$$\frac{du}{dt} = f(u, Ce^{-at}D^{1-\beta}(e^{at}w)), \qquad (9)$$

$$\frac{dw}{dt} = w_\infty(u) - \lambda e^{-at}D^{1-\alpha}(e^{at}w) - aw. \qquad (10)$$

Here, if $0 < \alpha \leq 1$, $D^{1-\alpha}$ is the fractional Riemann-Liouville derivative. If $\alpha > 1$, then $D^{1-\alpha} = I^{\alpha-1}$, known as the fractional Riemann-Liouville integral. The new parameters are α, β, λ and a. The parameter τ is not explicitly present in the fractional version, but generally, a and λ are inversely related to τ. If $\alpha = \beta = 1, a = 1/\tau, \lambda = 0$ and $w := w/\tau$, we recover the classical case.

2.2. Fractional adapted FHN model

The traditional FHN system's solution waveform shows a hyperpolarization that deviates from the typical myocyte cardiac action potential, potentially affecting the model's recovery properties. This hyperpolarization can be mitigated by an adjustment proposed in [5]:

$$\frac{du}{dt} = -Gu\left(1 - \frac{u}{u_{th}}\right)\left(1 - \frac{u}{u_p}\right) - \eta_1 uw, \qquad (11)$$

$$\frac{dw}{dt} = \eta_2\left(\frac{u}{u_p} - \eta_3 w\right) = \frac{\xi u - w}{\tau}. \qquad (12)$$

Using the gamma Mittag-Leffler PDF (3) as a memory kernel for the slow variable, we obtain from Eq. (9)-(10) the generalized fractional FHN model:

$$\frac{du}{dt} = -Gu\left(1 - \frac{u}{u_{th}}\right)\left(1 - \frac{u}{u_p}\right)$$
$$\quad - \eta_1 Cue^{-at}D^{1-\beta}(e^{at}w), \qquad (13)$$

$$\frac{dw}{dt} = \xi u - \lambda e^{-at}D^{1-\alpha}(e^{at}w) - aw. \qquad (14)$$

3. Results and discussion

In this section, we discuss the emergence of EADs in the general fractional model (13)-(14), as shown in Figure 1:
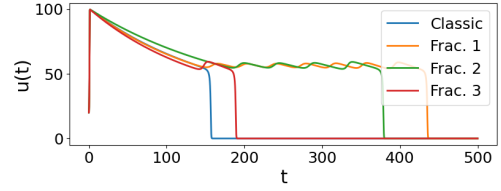

Figure 1. Examples of EADs generated with the model (13)-(14). Frac. 1 and Frac.2 are generated with simple gamma and Mittag-Leffler memory kernels, respectively.

3.1. The emergence of EADs in terms of mean and variance

Insights into the emergence of EADs can be gained when $\lambda = 0$ and $\alpha = 1$, representing a simple gamma memory kernel. This simplification allows for a focused study while preserving an important characteristic: by selecting $a = \mu/\sigma^2$ and $\beta = \mu^2/\sigma^2$ for any positive real values μ and σ^2, a kernel with the desired mean μ and variance σ^2 can be constructed.

In Figure 2A, the mean $\times$ variance plane is divided into three regions. From bottom to top, complete APs appear in the first region, ranging from Dirac delta memory kernels at the lower limit. The second region exhibits APs with EADs, and then there is a region of repolarization failure. Figure 2D depicts APs generated by the kernels in panel B, corresponding to the black vertical points in Figure 2A, illustrating changes in AP shape and repolarization difficulty as variance increases. APs in Figure 2E are generated by the kernels in panel C, corresponding to the black horizontal points in Figure 2A. Changes in AP shape when modifying the mean of the kernel are illustrated.

Transitioning from the dotted region without EADs to the red region with EADs can be achieved by slight adjustments to the left (lower mean) or upwards (higher variance). A leftward shift implies a shorter memory duration, while an upward shift maintains the mean but increases the variance, shifting the kernel towards the origin.

Biologically, EADs can arise from reduced repolarization reserve due to decreased outward current, increased inward current, or both, affecting the net outward current necessary for repolarization. In the FHN model, the fast variable represents transmembrane voltage, while the slow variable relates to potassium channel activation.

Shifting to the left or upwards in the mean $\times$ variance plane increases the dependence of the potassium current on recent voltage values, as the mode of the memory ker-
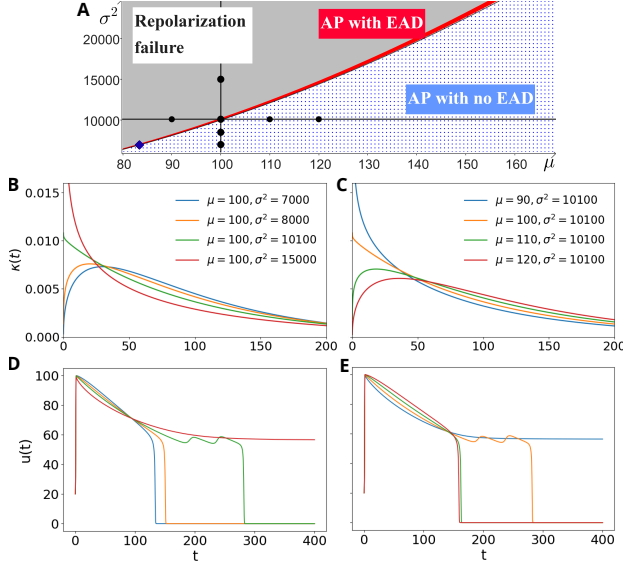
Figure 2. The blue diamond indicates a standard case. (A) Regions of normal AP, AP with EADs and repolarization failure. The black parabola corresponds to the integer cases. (B) Gamma kernels generated by the black points in panel A, going through the regions in a vertical slice. (C) Gamma kernels generated by the black points in panel A, going through the regions in a horizontal slice. (D) APs generated by the memory kernels in panel B. (E) APs generated by the memory kernels of panel C.

nel's PDF moves closer to the present. These adjustments lead to a premature decline in the potassium current response during repolarization, making the membrane more susceptible to reactivation by inward currents. It increases the likelihood of EADs and potential repolarization failure. An interesting observation is that during the initial stages of repolarization, the opposite effect occurs, as the potassium current reacts more promptly to voltage increases. Consequently, initial repolarization is accelerated when the mean of the slow variable is smaller or the variance is greater. This phenomenon is clearly illustrated in Figure 3. Panel B shows that the model from [1] has the same initial repolarization behavior.

Although the initial behavior is similar, it is important to note that the EAD mechanism differs. In the model by [1], EADs arise when the time constant of potassium gating is longer, despite the initial repolarization being slower. This second mechanism can also be explored in our model, as shown in the example Frac.2 of Figure 1, by incorporating memory kernels other than simple gamma kernels. Developing a general description of the emergence of EADs is challenging due to the diverse nature of general kernels, since not all of them can be accurately represented by a gamma kernel. For details on general gamma Mittag-
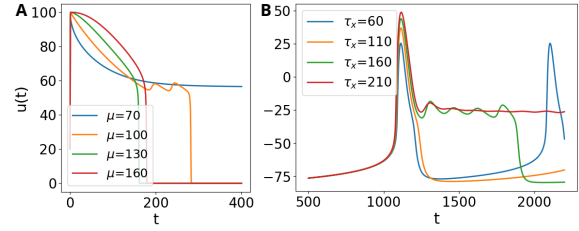

Figure 3. Initial repolarization is faster when the mean of the potassium-related variable is smaller. Panel A shows the presented model with a gamma memory kernel of fixed variance and mean μ, while panel B illustrates the same initial behavior of the model from [1], where τ_x is the time constant for potassium gating.

Leffler memory kernels, which can offer valuable insights into the influence of ion-channel shape memory on various types of EADs, refer to [6] and [2].

3.2. Stability analysis

From a stability analysis perspective, the transition from repolarization failure to a complete action potential is due to a change in stability. The use of fractional derivatives, which are non-autonomous, allows trajectories to self-intersect, enabling the generation of mixed-mode oscillations. Recent research (e.g., [7, 8]) suggests that oscillatory states emerge in fractional models near Hopf-like bifurcation points when a bifurcation parameter approaches a critical value. Replacing the Caputo fractional derivative in an integer model simplifies stability analysis, but in the constructive fractional system, it is challenging. Nevertheless, our findings indicate that EADs in the fractional generalized model result from an unstable focus or unstable limit cycles observed in the corresponding integer model.

The fractional system (13)-(14) exhibits the same equilibrium point as the corresponding integer system (11)-(12). In the integer model, a subcritical Hopf bifurcation occurs at a critical value τ^* (see Figure 4A). When τ slightly exceeds τ^*, the equilibrium point becomes an unstable spiral.

An unstable limit cycle emerges when τ is slightly less than τ^*, leading to the observation of EADs in the fractional model. For gamma memory kernels, setting $a = 1/\tau$ establishes a relationship between the mean and variance as $\mu/\sigma^2 = 1/\tau$. EADs occur when $\mu/\sigma^2 \approx 1/\tau^*$ and $\mu^2/\sigma^2 \approx \mu/\tau^* < 1$. Figure 4B shows a scenario with an unstable limit cycle in the integer model, where the equilibrium point is a stable spiral. The orange integer solution diverges from the green unstable limit cycle, while the blue integer solution follows a typical action potential shape. The fractional solution enters the spiral but can escape due to the trajectory's self-intersection capability.
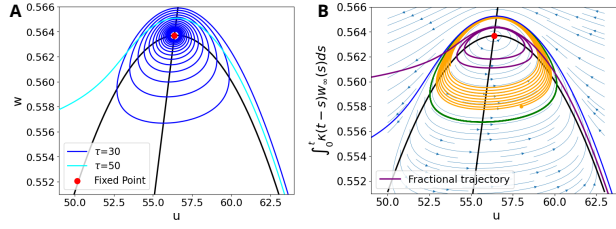
Figure 4. The nullclines of the integer-order model are depicted in black, and the red dot represents an equilibrium. Panel A presents phase portraits of solutions of the classic model (11)-(12) with $\tau < \tau^*$ and $\tau > \tau^*$. In Panel B, solutions of the classic model for τ slightly smaller than τ^* and different initial points are plotted, showing an unstable limit cycle. The orange dot indicates the initial point of the orange trajectory, which spirals inwards. A fractional purple solution entering and exiting the spiral is presented.

4. Conclusions

The emergence of EADs was investigated by modifying the memory kernel of the slow variable in simple two-variable models using tools from FC. Recent studies such as [2, 3, 9] have advanced constructive methods for fractional modeling, highlighting the role of fractional functions in waiting times and delay kernels. In this work, we developed a mathematical protocol to extend FHN-type equations with gamma Mittag-Leffler distributed delays to induce mixed-mode oscillations as EADs. Paper [6] also applied this method to Mitchell-Schaffer and Karma models, after adapting them to a proper geometry.

To analyze the relationship between the memory kernel and EADs, we studied changes in the mean and variance of the particular case of gamma kernels. Our findings indicate that transitioning from a state without EADs to one with EADs can be achieved by a slight decrease in the mean or a slight increase in the variance. These adjustments lead to a faster decrease in the potassium current response during repolarization, increasing the possibility of EADs. While these findings may not apply to all types of gamma Mittag-Leffler memory kernels, they provide a valuable starting point for future research.

We also observed that EADs occur when the fractional trajectory approaches an unstable spiral equilibrium or limit cycle of the integer-order system. The fractional trajectory can enter the spiral but has the ability to escape intersecting itself, due to the non-autonomous nature of fractional generalizations. The significance of spiral points in the formation of EADs aligns with previous findings, such as [10], who demonstrated in a Luo-Rudy cardiac model that EADs arise when the non-resting steady state of the voltage/Ca current subsystem loses stability through a Hopf bifurcation, leading to oscillations. Future work should focus on explicitly linking fractional parameters to experimental biomarkers to enhance the translational impact of this approach.

References

[1] Barrio R, Jover-Galtier JA, Martínez M, Pérez L, Serrano S. Mathematical birth of early afterdepolarizations in a cardiomyocyte model. Mathematical Biosciences 2023; 366:109088.

[2] Monteiro NZ, dos Santos RW, Mazorche SR. Bridging the gap between models based on ordinary, delayed, and fractional differentials equations through integral kernels. Proceedings of the National Academy of Sciences 2024; 121(19):e2322424121.

[3] Monteiro NZ, dos Santos RW, Mazorche SR. Constructive fractional models through Mittag-Leffler functions. Computational and Applied Mathematics 2024;43(4):177.

[4] Rameh RB, Cherry EM, dos Santos RW. Single-variable delay-differential equation approximations of the FitzHugh-Nagumo and Hodgkin-Huxley models. Communications in Nonlinear Science and Numerical Simulation 2020;82:105066.

[5] Franzone PC, Pavarino LF. A parallel solver for reaction–diffusion systems in computational electrocardiology. Mathematical models and methods in applied sciences 2004;14(06):883–911.

[6] Monteiro NZ, dos Santos RW, Mazorche SR. Ion channel memory drives cardiac early afterdepolarizations in fractional models. Mathematics 2025;13(10):1585.

[7] Gao XL, Zhang HL, Wang YL, Li ZY. Research on pattern dynamics behavior of a fractional vegetation-water model in arid flat environment. Fractal and Fractional 2024; 8(5):264.

[8] He K, Song J, Zhao N, Liu S. Hopf bifurcation and dynamical transitions in a fractional-order FitzHugh-Rinzel model with multiple time delays. Communications in Nonlinear Science and Numerical Simulation 2025;141:108471.

[9] Angstmann CN, Erickson AM, Henry BI, McGann AV, Murray JM, Nichols JA. A general framework for fractional order compartment models. SIAM Review 2021; 63(2):375–392.

[10] Tran DX, Sato D, Yochelis A, Weiss JN, Garfinkel A, Qu Z. Bifurcation and chaos in a model of cardiac early afterdepolarizations. Physical review letters 2009;102(25):258103.

Address for correspondence:

Noemi Zeraick Monteiro

Federal University of Juiz de Fora – Juiz de Fora – MG – CEP 36036-330 - Brazil

monteiro.zeraick@estudante.ufjf.br